



HAL
open science

Geometric modeling with small defects of over-constrained Parallel Kinematic Machine

Jean-Baptiste Guyon, H el ene Chanal, Benjamin Boudon, Beno t Blaysat

► **To cite this version:**

Jean-Baptiste Guyon, H el ene Chanal, Benjamin Boudon, Beno t Blaysat. Geometric modeling with small defects of over-constrained Parallel Kinematic Machine. Mechanism and Machine Theory, In press, 179, pp.105120. 10.1016/j.mechmachtheory.2022.105120 . hal-03820703

HAL Id: hal-03820703

<https://uca.hal.science/hal-03820703>

Submitted on 19 Oct 2022

HAL is a multi-disciplinary open access archive for the deposit and dissemination of scientific research documents, whether they are published or not. The documents may come from teaching and research institutions in France or abroad, or from public or private research centers.

L'archive ouverte pluridisciplinaire **HAL**, est destin ee au d ep ot et  a la diffusion de documents scientifiques de niveau recherche, publi es ou non,  emanant des  tablissements d'enseignement et de recherche fran ais ou  trangers, des laboratoires publics ou priv es.

Geometric modelling with small defects of over-constrained Parallel Kinematic Machine

Jean-Baptiste GUYON^a, H el ene CHANAL^a, Benjamin BOUDON^a, Beno t
BLAYSAT^a

^a*Universite Clermont Auvergne Clermont Auvergne INP CNRS Institut Pascal F-63000
Clermont-Ferrand France*

Abstract

In the case of over-constrained mechanisms, the system can only be assembled or move under strict geometric conditions. A crucial step is to identify these conditions from the geometric model. Classically, the geometric model of a robot is computed from the Denavit-Hartenberg formalism. However, when imperfect mechanisms are studied, this formalism does not introduce exhaustively small geometric defects. In this article, a formalism based on kinematic joint invariants is preferred to describe the geometric behavior. The efficiency of this formalism is demonstrated for the accuracy improvement of a serial robot. A stationarity analysis of the geometric model is then performed to determine the geometric constraints induced by the over-constrained systems and to reduce the number of geometric parameters initially introduced. The methodology is first illustrated on an over-constrained slider-rod-crank system. Then, it is applied to the over-constrained mechanism of the Tripteor X7, a Parallel Kinematic Machine-tool. The benefit of our methodology is validated by a comparison of the geometric model obtained with a CAD model and a previous geometric model proposed in the literature. Finally, the identification of the parameters of the defined geometric model is conducted in order to quantify the potential accuracy benefit.

Keywords:

identification, over-constrained mechanism, geometric model, geometric defects, stationarity analysis

1. Introduction

Parallel kinematics manipulators are now commonly used for machining. Indeed, the kinematic and dynamic capabilities of these kind of architecture can be relevant for High-Speed Machining (HSM) [1]. However, their level of accuracy is low compared to Serial Kinematic Machine-tool [2]. This limitation is due to the fact that the end-effector of Parallel Kinematic Machine-tool (PKM) is connected to the fixed platform with at least two independent kinematic chains [3].

To improve the accuracy of the end-effector pose (positioning and orientation) of a PKM, research works investigate particularly two ways: the increasing of stiffness and the improvement of geometric identification process [4]. To increase stiffness without weighting the PKM structure, over-constrained PKM were designed and developed [5]. An over-constrained PKM is defined as a PKM with common or redundant constraints that can be removed without changing the kinematics of the mechanism [6]. A stiffness comparison between Tricept robot and Tripteor X7 (an over-constrained PKM equivalent to Tricept in term of architecture and motion) shows a decrease of $0.177mm$ on average for the linear displacement induced by a $450N$ load [5]. This difference is important regarding machining requirement ($< 0.05mm$) [1].

However, over-constrained mechanism complicates the control of geometric behavior. Indeed, for example, the classic formula of Kutzbach-Grübler for computing the mobility of general spatial mechanisms does not always work in the case of over-constrained mechanism [7]. Thus, dedicated studies are required to improve accuracy of over-constrained PKM after an identification process.

Ramesh's work underlines the importance of a geometric identification in the case of robots with serial architecture [8]. This identification allows to reduce the geometric transformation errors. Majarena shows the importance of geometric identification for PKM in order to reach the target point in the workspace with greater accuracy [9]. In his work, the positioning errors are divided by a factor 10 and the orientation errors by a factor 20 after identification. The geometric identification is performed in four steps: modeling, measurement, identification and correction [10]. The geometric model that includes defects is the first step of this process.

The geometric model including defects is a mathematical description of the geometric behavior of the studied robot. This model expressed the end-effector pose in the fixed frame regarding the value of the active joints and

geometric defects. Two types of defects can be implemented in the geometric model of a robot [11]. The size defects are linked to the variation of the non-null size parameters introduced to describe the nominal geometry of a robot architecture. The other small defects concern all the other small variation which are defined to model the geometric behavior of a robot with a greater accuracy.

There is a challenge to determine the minimum number of geometric defects to be introduced in order to control the robustness of the identification process ([12] and [13]). Alici performs the identification of a serial structure with 14 and 18 parameters [14]. Models with fewer identified parameters lead to a larger residual error. However, increasing the number of parameters makes the model sensitive to identification errors [13]. It is therefore necessary to evaluate the relevance of all the parameters introduced in the model. The reduction of the number of parameters can be achieved by introducing only independent parameters related to the different links as in the work of Chen [15] and Everett [16] or through a sensitivity analysis as presented by Fan [17].

Considering of serial robots, the number C of independent geometric parameters necessary to define the geometric model is known according to [16]:

$$C = 4R + 2P + 6 \quad (1)$$

where R is the number of rotational joints and P is the number of prismatic joints. However, this formula can not be applied for over-constrained PKM. Indeed, an over-constrained PKM can only be assembled or move under strict geometric conditions [18]. These geometric conditions reduce the number of independent geometric parameters which should be introduced in the geometric model. The aim of this paper is to propose a methodology to determine the influence of over-constrained mechanisms on the number of geometric parameters necessary to establish the geometric model including defects of an over-constrained PKM with an attempted final accuracy less than $0.05mm$.

A classical method for defining geometric models of robots is based on the Denavit-Hartenberg (DH) formalism [19]. This formalism introduces length and angle parameters. However, this formalism is inadequate to model defects between two almost parallel adjacent joints due to the numerical instabilities that rise during the identification process [20]. In addition, it does not ensure to consider joint axis orientation defect on $(\overrightarrow{x_{i-1}}, \overrightarrow{z_{i-1}})$ plane (**Fig.1**). Moreover, the introduced geometric defects are of different natures (length

and angle) which contribute to the poor conditioning of the identification process [21].

To override the drawback of DH formalism, Chanal proposed a new formalism based on a vector description of kinematic joint invariants [11]. Currently, this formalism was uniquely apply to a SCARA robot. The application of this new formalism in case of the SCARA robot ensures to improve the final accuracy after an identification process in comparison to a model defined from DH formalism with small defects. In this article, an adaptation of this formalism to PKM is proposed. The initial number of introduced geometric defects respects equation (1). Thus, a stationarity study is conducted to identify the geometric parameters which must be null to guarantee the assembling and the moving of the studied over-constrained PKM if all its elements are considered as rigid. The present study ensures to reduce the number of geometric parameters necessary to model the geometric behavior of OPKM and appears as the basis on future studies about the deformation of the over-constrained mechanism during a motion when one of these geometric constraints is violated.

This article is organised into five sections. First, the formalism applied to define the geometric model of PKMs is introduced. Then, the methodology used to determine the geometric constraints imposed by an over-constrained mechanism is presented. This methodology is based on a stationnarity analysis. The next section shows the application of the method on two systems: an over-constrained slider-rod-crank mechanism and an over-constrained PKM, the Tripteor X7. Finally, the identification of the Tripteor X7 geometric parameters is presented to validate the potential accuracy benefit brought by the proposed approach.

2. Methodology for defining the imperfect geometric model with small defects

First, an initial geometric model including small defects is developed. This model must ensure a definition of an exhaustive geometric defects. Thus, we choose to apply a formalism based on a vector modeling of kinematic joint invariants [11]. In addition, robot's links are decomposed into 1 degree of freedom (DoF) links in order to decompose movement and geometric defects between those movements. For a single-axis rotation, the joint invariants are a straight-line (i.e. the axis of rotation) [22]. 4 parameters are introduced for describing this geometric feature, i.e. 2 parameters to define the straight-line

orientation and 2 parameters to define a point of this straight-line. For a unidirectional translation, the joint invariant is a straight-line parallel to the direction of the translation, i.e. 2 parameters to define the orientation of this line [22]. To apply this formalism to a solid with two links, $i - 1$ and i , three coordinate systems are defined (**Fig. 1**):

- R_{L_i} , this frame is fixed regarding link i . The normalized vector \vec{z}_{L_i} is along the axis vector of joint i .
- $R_{P_{i-1}}$, this frame is fixed regarding link i . This frame is defined from frame $R_{L_{i-1}}$ by applying the movement allowed by link $i - 1$.
- System functional frames. These frames are defined by the PKM integrator in the numerical controller. These frames are, in particular, the end effector frame and the fixed platform frame of the system.

Frame R_{L_i} is defined such that:

- the normalised vector \vec{z}_{L_i} is along the axis vector of joint i . Its coordinates in frame $R_{P_{i-1}}$ are (I_i, J_i, K_i) ;
- the normalised vector \vec{x}_{L_i} is supported by the common perpendicular between \vec{z}_{L_i} and $\vec{z}_{P_{i-1}}$;
- the normalised vector \vec{y}_{L_i} completes the coordinate system thanks to the right-hand rule;
- The position of the origin point can be anywhere in the joint axis. Concretely, it is chosen to simplify the calculation. Thus, the coordinates of vector $\overrightarrow{O_{P_{i-1}}O_{L_i}}$ are in frame $R_{P_{i-1}}$ and are denoted (A_i, B_i, C_i) . These coordinates in the R_{L_i} frame change to $(X_i = X_{in} + dx_i, Y_i = Y_{in} + dy_i, Z_i = Z_{in})$ where (X_{in}, Y_{in}, Z_{in}) are the nominal dimensions and (dx_i, dy_i) are position defects. There is no defect on the \vec{z}_{L_i} axis since it is the invariant for both joint type and we choose to set O_{L_i} in the plane (X_{in}, Y_{in}) for easiness reason.

Frame R_{P_i} is defined by a rotation around the axis \vec{z}_{L_i} or by a translation along the axis \vec{z}_{L_i} of the frame R_{L_i} (**Fig.2**). The rotation around the \vec{z}_{L_i} axis is parameterized with the angle θ_i . The translation along the \vec{z}_{L_i} axis is parameterized with the length x_i .

The mathematical link between the introduced frames is expressed by three types of homogeneous matrices:

- the geometric parameters matrices $\mathbf{D}_{P_{i-1}}^{L_i}$ express frame R_{L_i} in frame $R_{P_{i-1}}$ according to small geometric defects. This matrix defines a rigid transformation which integrates geometric defects;
- the motion matrices $\mathbf{M}_{L_i}^{P_i}$ express frame R_{P_i} in frame R_{L_i} ; This matrix defines the movement of the concerned joint;
- the configuration frame matrix \mathbf{T}_A^B express the robot frames R_B defined in the numerical controller in the previous frame R_A . This matrix defines a rigid transformation.

The configuration frame matrices are not constrained, i.e. there is no standardization for the definition of this type of matrices.

Fig. 1 illustrates the introduced frame with their associated parameters. The particular expression of geometric parameter matrices $D_{P_{i-1}}^{L_i}$ is also given in **Fig. 1**.

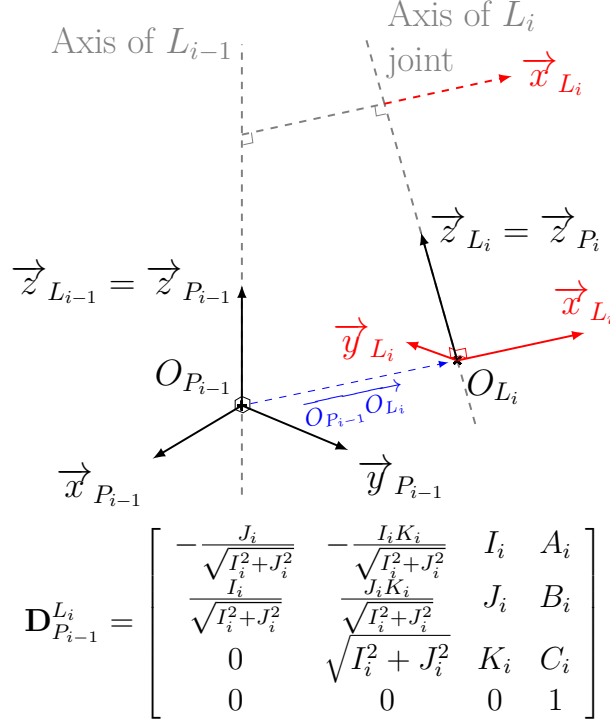


Figure 1: Definition of the frames and notations of the proposed formalism

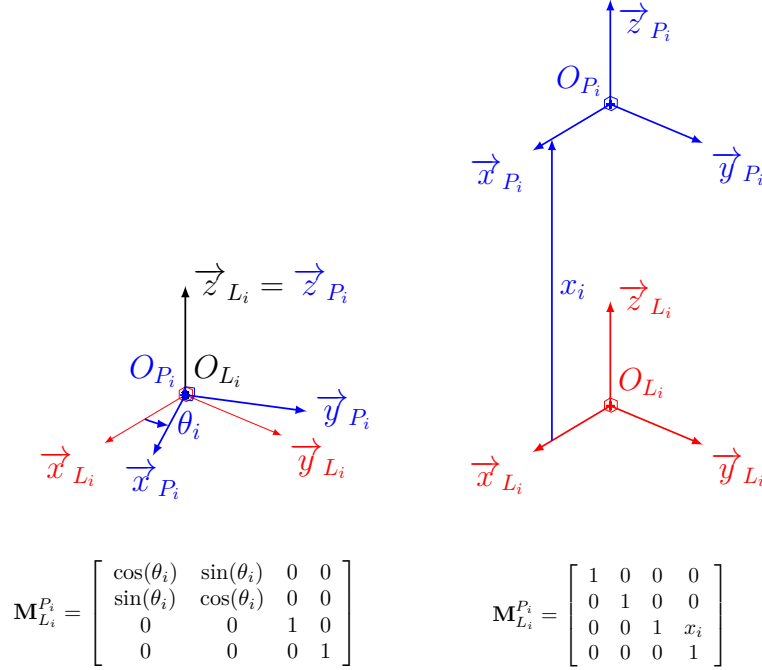


Figure 2: Definition of the necessary frames and matrices for the rotation and the translation movement

The system is decomposed into parallel or serial subsystems. Parallel subsystems are composed by several legs creating closed loops in the geometric model. Serial subsystems are simple links. The geometric model is realized from the product of the different defined matrices expressed for each leg as presented in the equation (2).

$$\mathbf{T}_{i0}^{P_F} = \mathbf{T}_0^{P_0} \cdot \left(\prod_{i=1}^N \mathbf{D}_{P_{i-1}}^{L_i} \cdot \mathbf{M}_{L_i}^{P_i} \right) \cdot \mathbf{T}_{P_N}^{P_F} \quad (2)$$

where $\mathbf{T}_{i0}^{P_F}$ expresses the final frame R_{P_F} in the reference frame R_{P_0} with the parameters of the concerned leg and both $\mathbf{T}_0^{P_0}$ and $\mathbf{T}_{P_N}^{P_F}$ are configuration frame matrices.

Thus, there are as many expressions of the matrix $\mathbf{T}_{i0}^{P_F}$ as legs of the parallel sub-system. The geometric model is obtained due to the equality of each expression.

To conclude this section, the model proposed introduces four parame-

ters per rotational joint: two position parameters since O_{P_i} and O_{L_i} are on the joint axis and two orientation parameters since \vec{z}_{L_i} is normalized ($\sqrt{I_i^2 + J_i^2 + K_i^2} = 1$). For a prismatic joint, two parameters are introduced: two orientation parameters since \vec{z}_{L_i} is normalized ($\sqrt{I_i^2 + J_i^2 + K_i^2} = 1$).

However, the geometric model defined in this section does not take into account the constraints on the geometric defects imposed by the over-constrained mechanism. The next section present a method to determine those constraints.

3. Stationarity analysis of an over-constrained mechanism

By stationarity study, we mean the differentiation of the geometric model with respect to each geometric parameter and each passive joint parameter. With this kind of study, the impact of a small variation of a geometric parameter on the passive joint motions is thus analyzed. For a given geometric parameter, if the computation of the passive joint motions is not successful, this means that the studied geometric parameter is constraint by the over-constrained nature of the mechanism. This analysis is conducted to identify geometric constraints caused by the over-constrained mechanism.

The stationarity S for the system defined by the geometric model $f(\xi_i, q_j) = 0$ is written as follows:

$$S(f) = \sum_i \frac{\partial f}{\partial \xi_i} d\xi_i + \sum_j \frac{\partial f}{\partial q_{p_j}} dq_{p_j} = 0 \quad (3)$$

where ξ_i are the geometric parameters of the model, $d\xi_i$ the associated defects, q_{p_j} the passive joint parameters, and dq_{p_j} the corresponding small variations. This study evaluates the influence of a small variation of a geometrical parameter on the configuration of the system with the hypothesis of small displacements.

This study is performed by considering no defect on the active joint positions. Thus, it ensures to focus on the influence of each geometric parameter variation on the mechanism movement. To the best of the author's knowledge, the stationarity study has not been exploited to study the particular geometric behaviour of over-constrained PKM.

This analysis helps determine constraints on geometric parameters of an over-constrained mechanism. Those constraints are the ones imposed to geometric parameters which must be respected to always verify $S = 0$. Failure to

meet these geometric constraints results in an unassemblable or not movable system.

In the following section, the method which ensures to identify the geometric constraint imposed by an over-constrained mechanism from the stationarity analysis is detailed.

4. Determination of geometric constraints

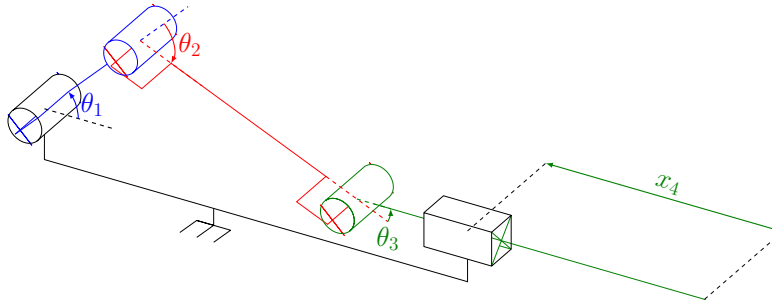
In this section, the proposed model and its associated stationarity analysis are performed on two over-constrained systems to determine the geometric constraints. The first system corresponds to an academic slider-rod-crank system. It serves as illustration of the method since this system is simple and well-known. The second studied system is the Tripteor X7, an over-constrained PKM.

4.1. 3D slider-rod-crank system

First, the method is applied on the slider-rod-crank system presented in the **Fig. 3**. This section presents in detail the complete method to identify geometric constraints of an over-constrained mechanism.

The introduced parameters respect the formalism presented in the above section. The definition of frames of the **Fig. 3** is realized according to the rules defined in section 2 as follow:

1. Frame R_{P_0} is the reference frame of the mechanism;
2. Frame R_{L_1} is defined such that $\vec{z}_{R_{L_1}}$ is along the revolution axis of the first link. Note that we choose $\vec{x}_{R_{L_1}}$ along $\vec{x}_{R_{P_0}}$;
3. Frame R_{R_1} is obtained from the rotation of frame R_{L_1} about angle $\vec{z}_{R_{L_1}}$ of θ_1 .
4. Frame R_{L_2} is defined such that $\vec{z}_{R_{L_2}}$ is along the revolution axis of the second joint. $\vec{x}_{R_{P_1}}$ is normal to $\vec{z}_{R_{L_1}}$ and $\vec{z}_{R_{L_2}}$;
5. Frame R_{R_2} is the rotation of frame R_{L_2} along $\vec{z}_{R_{L_2}}$ of angle θ_2 ;
6. Frame R_{L_3} is the translation of frame R_{R_2} along $\vec{x}_{R_{R_2}}$ in order to have $\vec{z}_{R_{L_3}}$ on the revolution axis of the third joint;
7. Frame R_{R_3} is the rotation of frame R_{L_3} along $\vec{z}_{R_{L_3}}$ of angle θ_3 ;
8. Frame R_{L_4} is the movement of frame R_{P_0} in order to have $\vec{z}_{R_{L_1}}$ on the translation axis of the fourth link and the origin of the frame R_{L_4} at the link location;
9. Frame R_{R_4} is the translation of frame R_{L_4} along $\vec{z}_{R_{L_4}}$ of length x_4 .



Kinematic model of slider-rod-crank mechanism

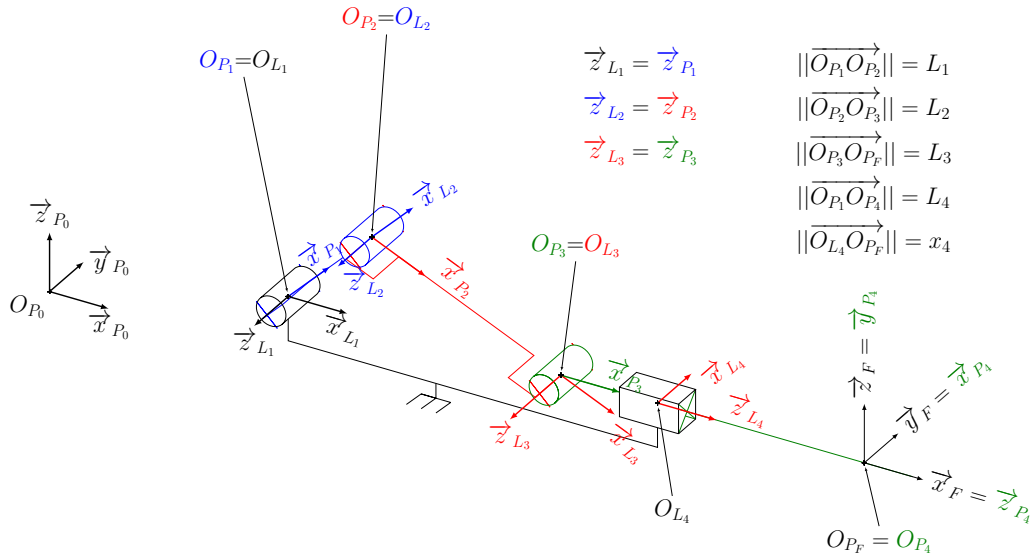


Figure 3: Parameterization of the slider-rod-crank mechanism

Nominal values of the introduced geometric parameters are given in **Table 1**. Note that in the case of the slide-rod-crank mechanism, A_i integrate size defects as they are size parameters with a non-null nominal value. Geometric parameter, motion and configuration frame matrices are given in equations (4),(5) and (6).

$$\begin{aligned}
D_{R_0}^{L_1} &= \begin{bmatrix} 1 & 0 & 0 & 0 \\ 0 & 0 & -1 & 0 \\ 0 & 1 & 0 & 0 \\ 0 & 0 & 0 & 1 \end{bmatrix} & D_{R_1}^{L_2} &= \begin{bmatrix} -\frac{J_2}{\sqrt{I_2^2+J_2^2}} & -\frac{I_2K_2}{\sqrt{I_2^2+J_2^2}} & I_2 & A_2 \\ \frac{I_2}{\sqrt{I_2^2+J_2^2}} & \frac{J_2K_2}{\sqrt{I_2^2+J_2^2}} & J_2 & B_2 \\ 0 & \sqrt{I_2^2+J_2^2} & K_2 & C_2 \\ 0 & 0 & 0 & 1 \end{bmatrix} \\
D_{R_2}^{L_3} &= \begin{bmatrix} -\frac{J_3}{\sqrt{I_3^2+J_3^2}} & -\frac{I_3K_3}{\sqrt{I_3^2+J_3^2}} & I_3 & A_3 \\ \frac{I_3}{\sqrt{I_3^2+J_3^2}} & \frac{J_3K_3}{\sqrt{I_3^2+J_3^2}} & J_3 & B_3 \\ 0 & \sqrt{I_3^2+J_3^2} & K_3 & C_3 \\ 0 & 0 & 0 & 1 \end{bmatrix} & D_{R_0}^{L_4} &= \begin{bmatrix} -\frac{J_4}{\sqrt{I_4^2+J_4^2}} & -\frac{I_4K_4}{\sqrt{I_4^2+J_4^2}} & I_4 & A_4 \\ \frac{I_4}{\sqrt{I_4^2+J_4^2}} & \frac{J_4K_4}{\sqrt{I_4^2+J_4^2}} & J_4 & B_4 \\ 0 & \sqrt{I_4^2+J_4^2} & K_4 & C_4 \\ 0 & 0 & 0 & 1 \end{bmatrix}
\end{aligned} \tag{4}$$

$$\begin{aligned}
M_{L_1}^{R_1} &= \begin{bmatrix} \cos(\theta_1) & -\sin(\theta_1) & 0 & 0 \\ \sin(\theta_1) & \cos(\theta_1) & 0 & 0 \\ 0 & 0 & 1 & 0 \\ 0 & 0 & 0 & 1 \end{bmatrix} & M_{L_2}^{R_2} &= \begin{bmatrix} \cos(\theta_2) & -\sin(\theta_2) & 0 & 0 \\ \sin(\theta_2) & \cos(\theta_2) & 0 & 0 \\ 0 & 0 & 1 & 0 \\ 0 & 0 & 0 & 1 \end{bmatrix} \\
M_{L_3}^{R_3} &= \begin{bmatrix} \cos(\theta_3) & -\sin(\theta_3) & 0 & 0 \\ \sin(\theta_3) & \cos(\theta_3) & 0 & 0 \\ 0 & 0 & 1 & 0 \\ 0 & 0 & 0 & 1 \end{bmatrix} & M_{L_4}^{R_4} &= \begin{bmatrix} 1 & 0 & 0 & 0 \\ 0 & 1 & 0 & 0 \\ 0 & 0 & 1 & x_4 \\ 0 & 0 & 0 & 1 \end{bmatrix}
\end{aligned} \tag{5}$$

$$T_{R_3}^{R_F} = \begin{bmatrix} 1 & 0 & 0 & L_3 \\ 0 & 0 & 1 & 0 \\ 0 & -1 & 0 & 0 \\ 0 & 0 & 0 & 1 \end{bmatrix} \quad T_{R_4}^{R_F} = \begin{bmatrix} 0 & 1 & 0 & 0 \\ 0 & 0 & 1 & 0 \\ 1 & 0 & 0 & 0 \\ 0 & 0 & 0 & 1 \end{bmatrix} \tag{6}$$

15 geometric parameters, including defects, are introduced: 9 for the orientation of joints axis ($I_2, J_2, K_2, I_3, J_3, K_3, I_4, J_4, K_4$) and 6 for the position of the joint axis ($A_2, B_2, C_2, A_3, B_3, C_3$). Note that a part of these parameters are dependant since \vec{z}_{L_i} is a normalized vector and since O_{P_i} and O_{L_i} are on the joint axis.

In this system, the input motion is defined by the active angle parameter θ_1 and the output motion is defined by the passive length parameter x_4 (**Fig.3**).

The system equation obtained by the closure of the kinematic loop is given in equation (7).

$$T_1 \begin{smallmatrix} R_F \\ R_0 \end{smallmatrix} = \mathbf{D}_{R_0}^{L_1} \mathbf{M}_{L_1}^{R_1} \mathbf{D}_{R_1}^{L_2} \mathbf{M}_{L_2}^{R_2} \mathbf{D}_{R_2}^{L_3} \mathbf{M}_{L_3}^{R_3} T_{R_3}^{R_F} = \mathbf{D}_{R_0}^{L_4} \mathbf{M}_{L_4}^{R_4} T_{R_4}^{R_F} = T_2 \begin{smallmatrix} R_F \\ R_0 \end{smallmatrix} \quad (7)$$

where $T_1 \begin{smallmatrix} R_F \\ R_0 \end{smallmatrix}$ is the matrix linking the reference frame to the final frame passing by parts 1, 2, 3 and 4 and $T_2 \begin{smallmatrix} R_F \\ R_0 \end{smallmatrix}$ is the matrix linking the reference frame to the final frame passing by parts 0 and 4.

Table 1: Nominal parameters for the slider-rod-crank mechanism

i	I_i	J_i	K_i	A_i	B_i	C_i
1	0	-1	0	0	0	0
2	0	0	1	L_1	0	0
3	0	0	1	L_2	0	0
4	1	0	0	L_4	0	0

The stationarity methodology proposed in equation (3) is also applied on the orthonormalization constraint equations of joint R_{L_i} : $I_i^2 + J_i^2 + K_i^2 = 1$. These equations give the relations $I_i \times dI_i + J_i \times dJ_i + K_i \times dK_i = 0$. Since the considered joints are only revolute or prismatic joints, the variations of the joint axis along the \vec{z}_{L_i} axis are not constrained by an over-constrained mechanism. In the slider-rod-crank system presented, this leads to $dK_2 = 0$, $dK_3 = 0$ and $dI_4 = 0$ since $I_2 = J_2 = 0$, $I_3 = J_3 = 0$ and $J_4 = K_4 = 0$.

The stationary analysis of the obtained geometric model gives twelve equations. Nine of them strictly concern the defects associated to orientation parameters. The three left over deal with the defects associated to position and orientation parameters. In the nine equations concerning orientation constraints, some are linear combination of others. This system of equations can be reduced to six independent equations. The system (8) consists of the independent equations extracted from the stationarity analysis of the geometric model. The study of those equations ensures the determination of several geometric constraints of the over-constrained system.

$$\left\{ \begin{array}{l}
eq_I = -\sin(\theta_1)dJ_2 - \cos(\theta_1)dI_3 - dJ_4 - \sin(\theta_3)dJ_3 = 0 \\
eq_{II} = -dK_4 - \frac{dI_3}{J_3} - \frac{dI_2}{J_2} - \frac{\cos(\theta_2) - \cos(\theta_1 - \theta_3)}{2} J_3 dI_2 = 0 \\
eq_{III} = dJ_4 + (\cos(\theta_3) - \cos(\theta_1))dI_2 + \cos(\theta_3)dI_3 \\
+ \sin(\theta_3)dJ_3 + \sin(\theta_1)dJ_2 = 0 \\
eq_{IV} = -(\sin(\theta_3) + \sin(\theta_1))dI_2 + \cos(\theta_3)dJ_3 \\
- \sin(\theta_3)dI_3 - \cos(\theta_1)dJ_2 = 0 \\
eq_V = dK_4 + \frac{dI_3}{J_3} + \frac{dI_2}{J_2} = 0 \\
eq_{VI} = \cos(\theta_1)dJ_2 - \sin(\theta_1)dI_3 - \cos(\theta_3)dJ_3 = 0 \\
eq_{VII} = -\sin(\theta_3)db_3 - dX_4 + \frac{L_2 \sin(\theta_3)}{J_2} dI_2 + \\
\cos(\theta_1)da_2 + \cos(\theta_1)da_3 - \sin(\theta_1)db_2 \\
+ L_2 \sin(\theta_3)d\theta_3 = 0 \\
eq_{VIII} = -(L_3 \sin(\theta_1) + L_2 \sin(\theta_2))dJ_2 - dc_2 - (L_3 + x_4 + L_4)dJ_4 \\
- L_3 \cos(\theta_1)dI_3 - L_3 \sin(\theta_3)dJ_3 = 0 \\
eq_{IX} = -(L_3 + x_4 + L_4)dK_4 - \cos(\theta_3)db_3 + \cos(\theta_1)db_2 + \sin(\theta_1)da_2 \\
+ \sin(\theta_1)da_3 - \frac{L_3}{J_2} dI_2 - \frac{L_3}{J_3} dI_3 + L_2 \cos(\theta_3)d\theta_3 \\
- \frac{J_3 L_3 \cos(\theta_2)}{2} dI_2 \\
+ \frac{L_2 \cos^2(\theta_3)}{J_2} dI_2 + \frac{J_3 L_3 \cos(\theta_1 - \theta_3)}{2} dI_2 = 0
\end{array} \right. \quad (8)$$

Step by step, the necessary conditions that the geometric parameter defects shall satisfy to guarantee the validity of equation I to equation IX are studied. For example, since the nominal value of J_2 and J_3 are equals to zero (**Table 1**), the defect dI_3 and dI_2 are equal to zero to avoid eq_{II} tending to infinity. By taking into account the zero value of dI_2 and dI_3 in eq_V , $dK_4 = 0$ is obtained. In addition, $d\theta_1$ and $d\theta_3$ can reach different values for each configuration of the system. These values can be determined to guarantee that system of equations (8) is satisfied. Thus, from eq_{IV} and eq_{VI} , by taking into account that $dI_2 = dI_3 = 0$, dJ_2 and dJ_3 need to be equal to zero. Finally, replacing those results in system of equations (8) gives two last constraints:

$dJ_4 = 0$ and $dc_2 = 0$.

This study on the slider-rod-crank system gives a total of 6 constraints on 6 defects associated to orientation parameters and one constraint on a defect associated to a position parameter. In other words, the stationary study ensures to find 6 geometric constraints on 6 defects which are dI_2 , dJ_2 , dI_3 , dJ_3 , dJ_4 , dK_4 and dc_2 shall be equal to zero. Those constraints show the need of the slider-rod-crank system to be planar as it is expected for this well-known system. In addition, from the 15 parameters introduced in the proposed geometric model, 9 parameters can take value different to 0 to guarantee the assembly and the movement of the system.

In this section, the model and the stationnarity analysis have been applied on the slider-rod-crank system in order to present the complete method on a simple and well-known system. The next part of this article focus on an over-constrained PKM: the Tripteor X7.

4.2. Tripteor X7 PKM

The Tripteor X7 is an over-constrained PKM whose kinematic model is presented in **Fig.4**. Frames used in the model of the Tripteor X7 are set up in the same way than the slider-rod-crank system previously presented. Note that frame R_{ICS} is the frame of the fixed platform and frame R_{MPS} is the frame of the mobile platform (**Fig.7**). The approach is divided in four sub-system presented in equation (9) :

$$\left\{ \begin{array}{l} \mathbf{T}_{1 \ ICS}^{MPS} = \mathbf{D}_{ICS}^{L11} \mathbf{M}_{L11}^{R11} \mathbf{D}_{R11}^{L21} \mathbf{M}_{L21}^{R21} \mathbf{D}_{R21}^{L41} \mathbf{M}_{L41}^{R41} \\ \quad \mathbf{D}_{R41}^{L51} \mathbf{M}_{L51}^{R51} \mathbf{T}_{R51}^{MPS} \\ \mathbf{T}_{2 \ ICS}^{MPS} = \mathbf{D}_{ICS}^{L12} \mathbf{M}_{L12}^{R12} \mathbf{D}_{R12}^{L22} \mathbf{M}_{L22}^{R22} \mathbf{D}_{R22}^{L32} \mathbf{M}_{L32}^{R32} \\ \quad \mathbf{D}_{R32}^{L42} \mathbf{M}_{L42}^{R42} \mathbf{D}_{R42}^{L52} \mathbf{M}_{L52}^{R52} \mathbf{D}_{R52}^{L51} \mathbf{T}_{R51}^{MPS} \\ \mathbf{T}_{3 \ ICS}^{MPS} = \mathbf{D}_{ICS}^{L13} \mathbf{M}_{L13}^{R13} \mathbf{D}_{R13}^{L23} \mathbf{M}_{L23}^{R23} \mathbf{D}_{R23}^{L43} \mathbf{M}_{L43}^{R43} \\ \quad \mathbf{D}_{R43}^{L53} \mathbf{M}_{L53}^{R53} \mathbf{D}_{R53}^{L51} \mathbf{T}_{R51}^{MPS} \\ \mathbf{T}_{MPS}^T = \mathbf{D}_{MPS}^{L6} \mathbf{M}_{L6}^{R6} \mathbf{D}_{R6}^{L7} \mathbf{M}_{L7}^{R7} \mathbf{T}_{R7}^T \end{array} \right. \quad (9)$$

with:

- $\mathbf{T}_{1 \ ICS}^{MPS}$ the model for the first leg (**Fig.5 a**));
- $\mathbf{T}_{2 \ ICS}^{MPS}$ the model for the second leg (**Fig.5 b**));

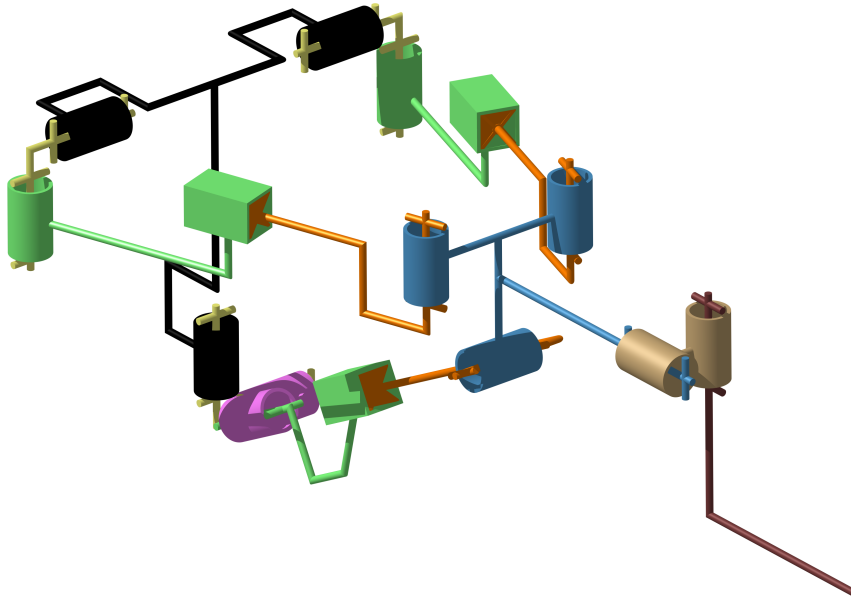


Figure 4: Kinematic model of the Tripteor X7, the black part corresponds to the fixed platform, the cyan part to the mobile platform and the dark brown hosts the spindle of the machine-tool

- $\mathbf{T}_3^{MPS}_{ICS}$ the model for the third leg (**Fig.5 c**);
- \mathbf{T}_{MPS}^T the model of the wrist of the Tripteor X7 (from the platform MPS to the tool T).

75 defects associated to 75 geometric parameters are introduced in the model of the machine parallel architecture and are referenced in the **Table 2**.

The application of the stationarity analysis on the normalization equation of \vec{z}_{L_i} vectors constraints gives 14 constraints on defects parameters: the variations of the joint axis along the \vec{z}_{L_i} axis is not constrained by the over-constrained mechanism. In order to write the closure properties of the over-constraint parallel architecture of the machine, two loops are considered by subtracting sub-system matrices defined in equations (9): $\mathbf{T}_1^{MPS}_{ICS} - \mathbf{T}_2^{MPS}_{ICS} = 0$ and $\mathbf{T}_1^{MPS}_{ICS} - \mathbf{T}_3^{MPS}_{ICS} = 0$. The stationarity analysis is applied to the geometric model expressed thanks to these two equations.

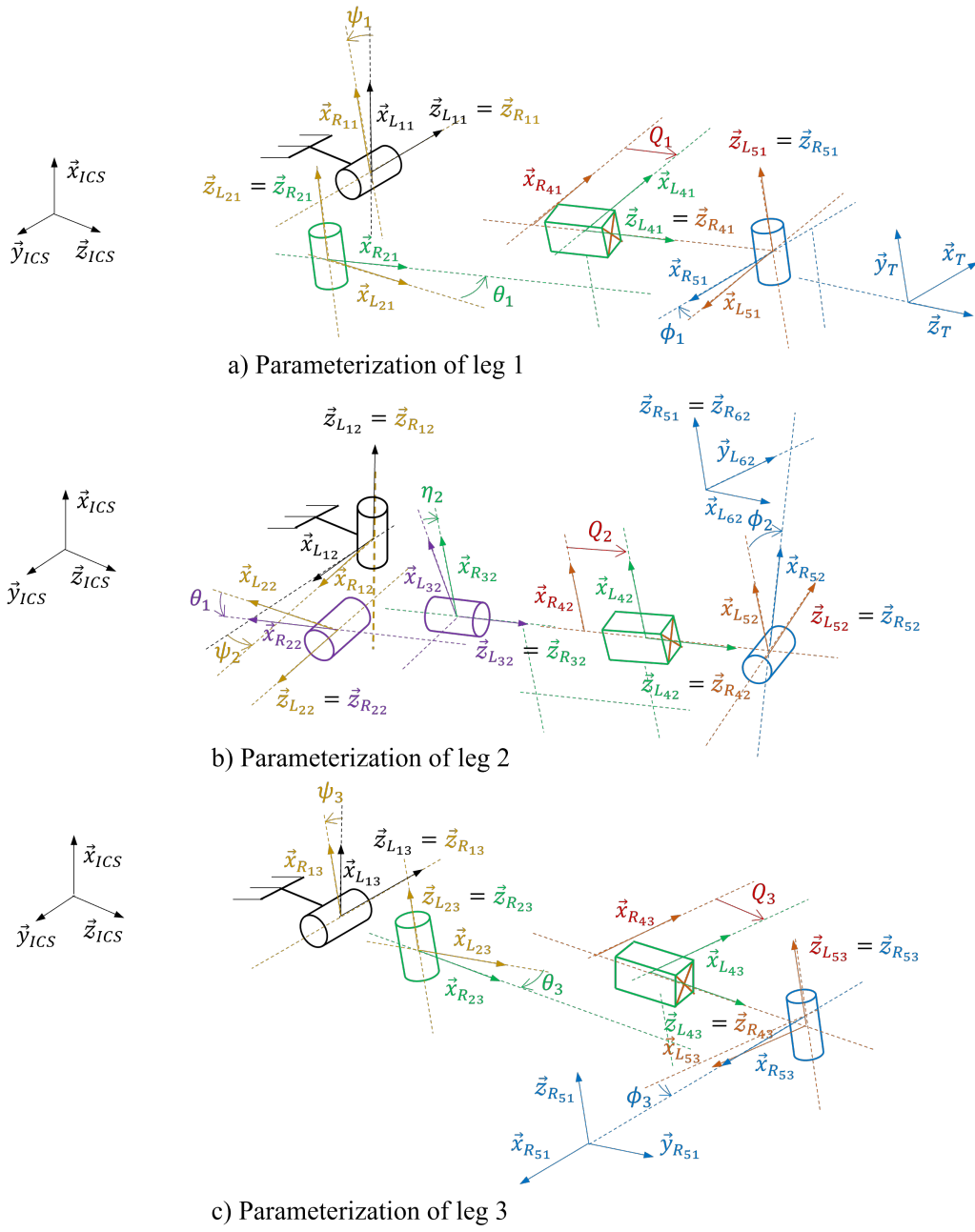


Figure 5: Parameterization of the Tripteor X7 legs

Leg 1	\mathbf{D}_{ICS}^{L11}	\mathbf{D}_{R11}^{L21}	\mathbf{D}_{R21}^{L41}	\mathbf{D}_{R41}^{L51}		
	\times	dI_{21}	dI_{41}	dI_{51}		
	\times	dJ_{21}	dJ_{41}	dJ_{51}		
	\times	dK_{21}	dK_{41}	dK_{51}		
	\times	da_{21}	\times	da_{51}		
	\times	db_{21}	\times	db_{51}		
	\times	dc_{21}	\times	dc_{51}		
Leg 2	\mathbf{D}_{ICS}^{L12}	\mathbf{D}_{R12}^{L22}	\mathbf{D}_{22}^{L32}	\mathbf{D}_{R32}^{L42}	\mathbf{D}_{R42}^{L52}	\mathbf{D}_{R52}^{R51}
	dI_{12}	dI_{22}	dI_{32}	dI_{42}	dI_{52}	dI_{62}
	dJ_{12}	dJ_{22}	dJ_{32}	dJ_{42}	dJ_{52}	dJ_{62}
	dK_{12}	dK_{22}	dK_{32}	dK_{42}	dK_{52}	dK_{62}
	da_{12}	da_{22}	da_{32}	\times	da_{52}	da_{62}
	db_{12}	db_{22}	db_{32}	\times	db_{52}	db_{62}
	dc_{12}	dc_{22}	dc_{32}	\times	dc_{52}	dc_{62}
Leg 3	\mathbf{D}_{ICS}^{L13}	\mathbf{D}_{R13}^{L23}	\mathbf{D}_{R23}^{L43}	\mathbf{D}_{R43}^{L53}	\mathbf{D}_{R53}^{R51}	
	dI_{13}	dI_{23}	dI_{43}	dI_{53}	dI_{63}	
	dJ_{13}	dJ_{23}	dJ_{43}	dJ_{53}	dJ_{63}	
	dK_{13}	dK_{23}	dK_{43}	dK_{53}	dK_{63}	
	da_{13}	da_{23}	\times	da_{53}	da_{63}	
	db_{13}	db_{23}	\times	db_{53}	db_{63}	
	dc_{13}	dc_{23}	\times	dc_{53}	dc_{63}	

Table 2: 75 parameters introduced to model the Tripteor X7 parallel architecture

The application of the stationnarity on the first loop allows to find the first geometric constraints. The list of geometric constraints is extended with the application of the stationnarity on the second loop. A third application on the loop containing leg 2 and leg 3 confirms the determined constraints gathered in **Table 3**. To validate our approach, we choose to analyse the consistency of the obtained geometric constraints with the geometric model implemented in the numerical controller of the Tripteor X7.

Comparison of the determined constraints with other models

In order to evaluate the consistency of the geometric constraints found analytically, a CAD model of the Tripteor X7 skeleton is realized. The obtained constraints are moreover compared with the one expressed in Putch-

Leg 1	Leg 2	Leg 3
$dI_{21} = 0$	$dI_{12} = 0$	$dI_{13} = 0$
$dK_{21} = 0$	$dI_{22} = 0$	$dJ_{13} = 0$
$dI_{41} = 0$	$dI_{32} = 0$	$dK_{13} = 0$
$dK_{41} = 0$	$dI_{42} = 0$	$dI_{23} = 0$
$dI_{51} = 0$	$dJ_{42} = 0$	$dK_{23} = 0$
$dJ_{51} = 0$	$dK_{42} = 0$	$dI_{43} = 0$
$dK_{51} = 0$	$dJ_{52} = 0$	$dK_{43} = 0$
	$dK_{52} = 0$	$dI_{53} = 0$
	$dI_{62} = 0$	$dJ_{53} = 0$
	$dK_{62} = 0$	$dK_{53} = 0$
		$dI_{63} = 0$
		$dJ_{63} = 0$
		$dK_{63} = 0$

Table 3: Constraints due to hyperstatism for the Tripteor X7

ler’s work. Putchler’s work is the based of the definition of the geometric model implemented in the numerical controller of the Tripteor X7 PKM [23].

The CAD model of the Tripteor X7 skeleton is implemented in the Catia V5R21 software The geometric defect markers are introduced with the same definition introduced in the matrix of the **Fig. 1**. However, identity matrices are set up when two links are parallel, because the software performs approximations. Without this modification, the software returns errors for two parallel links. The active motion available at each joint is defined with the distance or angle constraints. The skeleton model is presented in **Fig. 6**.

Several defects are tested on the model and we gather three main behaviors from the software:

- The defect introduced creates an error from the software. It is impossible with this defect to reconfigure the machine because of its over-constrained structure;
- The defect introduced creates a movement of passive joints. The software generates a reconfiguration of the structure;
- The defect introduced changes nothing on the structure. The defect is not influent.

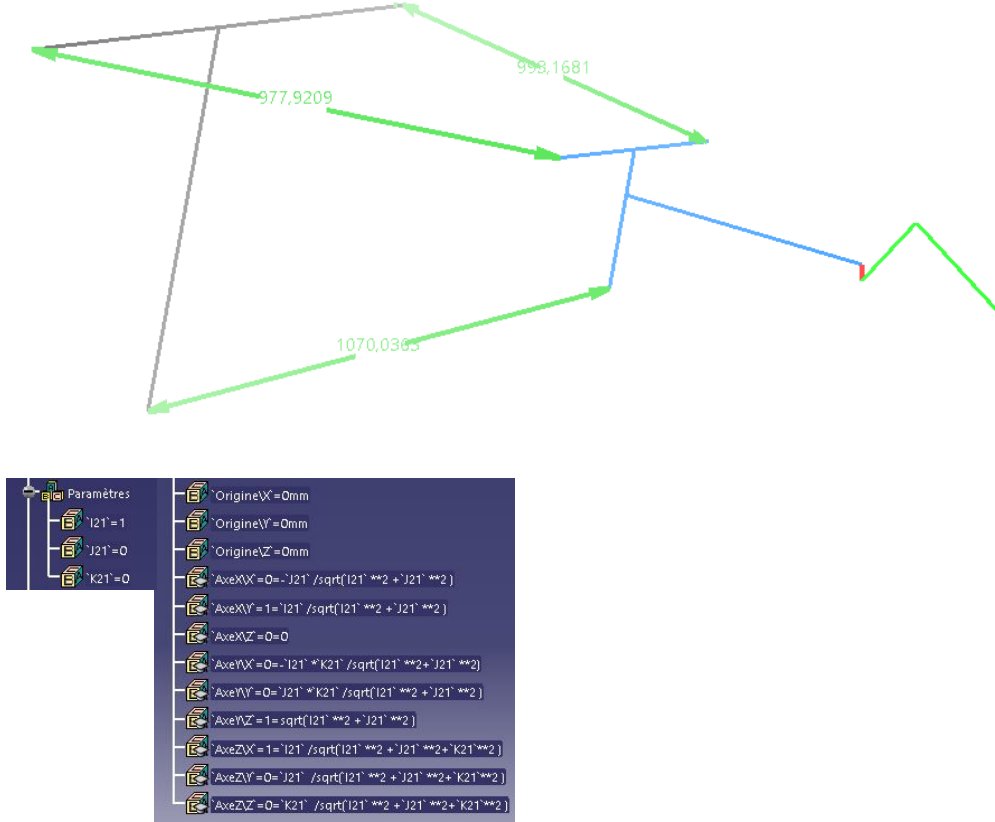


Figure 6: CAD model of the Tripteor X7 skeleton

The first and the third behavior are obtained when the defect studied is in **Table 3**. The second behavior occurs when there is no geometric constraints in the studied parameter.

On The other hand, Putschler's model [23] is the geometric model implemented in the numerical controller of the Tripteor X7. It is presented in the figure **Fig. 7**. The obtained geometric constraints are consistent with the Putschler's hypothesis except for 3 (**Table 4**). Actually, Putschler over-constrained the orientation of 3 rotational joints axes of the leg 2 (\vec{u}_2 , \vec{u}'_2 and \vec{v}_2). Putschler's model over-constrained the geometrical parameters which have an impact to the accuracy reached after an identification process and to the cost of the PKM.

In the next section, the proposed geometric model is applied, with its

Putchler model	Transcription of Putchler model in the model	Geometric constraints determined by the model presented and the stationnarity study
$\overrightarrow{u_1} // \overrightarrow{u_3}$	$\overrightarrow{z_{R11}} // \overrightarrow{z_{R13}}$	$dI_{13} = dK_{13} = 0$
$\overrightarrow{A_1 A_3} = \lambda \overrightarrow{u_1}$	$\overrightarrow{A_1 A_3} = L \cdot \overrightarrow{z_{R11}}$	Given by model
$\overrightarrow{u_1} \perp \overrightarrow{v_1}$ $\overrightarrow{u_3} \perp \overrightarrow{v_3}$	$\overrightarrow{z_{R11}} \perp \overrightarrow{z_{R21}}$ $\overrightarrow{z_{R13}} \perp \overrightarrow{z_{R23}}$	perpendicularity given by $dK_{21} = dK_{23} = 0$
$\overrightarrow{u_2} \perp \overrightarrow{v_2}$	$\overrightarrow{z_{R12}} \perp \overrightarrow{z_{R22}}$	\emptyset
$\overrightarrow{v_1} // \overrightarrow{w_1}$ $\overrightarrow{v_3} // \overrightarrow{w_3}$	$\overrightarrow{z_{R21}} // \overrightarrow{z_{R51}}$ $\overrightarrow{z_{R23}} // \overrightarrow{z_{R53}}$	Defects compensing themselves outside of the plane perpendicularity to $\overrightarrow{z_{R2i}}$ and $\overrightarrow{z_{R5i}}$ between R_{2i} et R_{5i} , $i \in \{1, 3\}$
$\overrightarrow{A''_i B_i} \perp \overrightarrow{v'_i}$	$\overrightarrow{A''_i B_i} \perp \overrightarrow{z_{R2i}}$	perpendicularity given by $dK_{4i} = 0$, $i \in \{1, 3\}$
$\overrightarrow{A''_i B_i} \perp \overrightarrow{w'_i}$	$\overrightarrow{A''_i B_i} \perp \overrightarrow{z_{R5i}}$	perpendicularity given by $dK_{5i} = 0$, $i \in \{1, 3\}$
$\overrightarrow{u'_2} \perp \overrightarrow{v'_2}$	$\overrightarrow{z_{R32}} \perp \overrightarrow{z_{R22}}$	\emptyset

Table 4: Comparison of determined geometric constraints with Putchler’s model hypothesis [23]

geometric constraints of the Tripteur X7, to illustrate its potential benefit in term of geometrical accuracy after an identification process.

5. Model identification

In order to illustrate the gain in term of accuracy of our approach, an identification of the model of Tripteur X7 is conducted. Measurements were done with a laser tracker in the workspace of the machine . **Fig. 8** presents the set of the 107 measured points in the workspace of the Tripteur X7.

According to the stationary analysis developed in the previous section, only 46 parameters have to be identified for the parallel architecture of the machine instead of 75. In addition, only 8 parameters have to be identified

for the serial wrist of the machine. These 52 parameters are gathered in the **Table 5**. They have to be identified to establish the geometric model of the complete structure of the PKM.

	<i>I</i>	<i>J</i>	<i>K</i>	<i>A</i>	<i>B</i>	<i>C</i>	Total
Leg 1	–	–	–	–	–	–	8
	–	<i>J</i> ₂₁	–	<i>A</i> ₂₁	<i>B</i> ₂₁	<i>C</i> ₂₁	
	–	<i>J</i> ₄₁	–	–	–	–	
	–	–	–	<i>A</i> ₅₁	<i>B</i> ₅₁	<i>C</i> ₅₁	
Leg 2	–	<i>J</i> ₁₂	<i>K</i> ₁₂	<i>A</i> ₁₂	<i>B</i> ₁₂	<i>C</i> ₁₂	24
	–	<i>J</i> ₂₂	<i>K</i> ₂₂	<i>A</i> ₂₂	<i>B</i> ₂₂	<i>C</i> ₂₂	
	–	<i>J</i> ₃₂	<i>K</i> ₃₂	<i>A</i> ₃₂	<i>B</i> ₃₂	<i>C</i> ₃₂	
	–	–	–	–	–	–	
	<i>I</i> ₅₂	–	<i>K</i> ₅₂	<i>A</i> ₅₂	<i>B</i> ₅₂	<i>C</i> ₅₂	
	–	<i>J</i> ₆₂	–	<i>A</i> ₆₂	<i>B</i> ₆₂	<i>C</i> ₆₂	
Leg 3	–	–	–	<i>A</i> ₁₃	–	<i>C</i> ₁₃	14
	–	<i>J</i> ₂₃	–	<i>A</i> ₂₃	<i>B</i> ₂₃	<i>C</i> ₂₃	
	–	<i>J</i> ₄₃	–	–	–	–	
	–	–	–	<i>A</i> ₅₃	<i>B</i> ₅₃	<i>C</i> ₅₃	
	–	–	–	<i>A</i> ₆₃	<i>B</i> ₆₃	<i>C</i> ₆₃	
Wrist	–	–	–	<i>A</i> ₆	<i>B</i> ₆	–	8
	<i>I</i> ₇	–	<i>K</i> ₇	<i>A</i> ₇	<i>B</i> ₇	<i>C</i> ₇	

Table 5: List of parameters to identify with the model presented

The identification process is conducted according to the graph in **Fig. 9**. The `lsqnonlin` function of the MatLab[®] software is used to minimize the cost function defined as follow:

$$f_{cost}(\xi_j) = \sum_{i=1}^{52} (\mathbf{X}_i - GM(Q_i, \xi_j))^2 \quad (10)$$

where \mathbf{X}_i are the measured positions and $GM(Q_i, \xi_j)$ is the Inverse Geometric Model in which ξ_j are geometric parameters with defects and Q_i are actuator position.

The rank of the Jacobian matrix of the optimisation is 52 as the numbers of parameters. However its conditioning is above 10^5 which is due to the low number of measured points.

The graph in **Fig. 10** presents the residual evaluations of f_{cost} . Despite the reduced number of measurement points, the positioning error of the end effector is decreased to less than $0.1mm$. Since the modification of the geometric model implemented in the numerical controller of Tripteor X7 is not possible, the validation of the accuracy of our geometric model is realized thanks to the measure of 30 other points (**Fig. 8**). The errors between the simulated position of these points with our identified model and the measures done by the laser tracker feature a maximum about $77.9\mu m$ and an average about $44.1\mu m$.

These values are consistent with machining applications.

6. Conclusion

Over-constrained structure are used to increase PKM stiffness. However, over-constrained mechanisms complexify the definition of the geometric model. Classical Denavit-Hartenberg [19] can be apply to model those over-constraint machines. However, the model introduced in this article presents the advantage of introducing the minimum number of necessary parameter to exhaustively describe the geometric behavior of over-constraint structures. The stationarity analysis allows identifying the geometric constraints due to over-constrained mechanism.

Two systems are modeled with the presented method: the well known slider-rod-crank system and the Tripteor X7 PKM. Geometric constraints are obtained with this method for both systems. Our methodology is unbiased and seems to be more robust compared to other works which identify geometric constraints thanks to an analysis based uniquely on their knowledge [23]. Since the introduced geometric parameters are exhaustively control, the final accuracy obtained after identification is improved.

Future works will be conducted to systemize the analysis of the stationarity study. Indeed, the rules and conclusions are extracted thanks to manual analysis.

References

- [1] H. Chanal, E. Duc, P. Ray, A study of the impact of machine tool structure on machining processes, International Journal of Machine Tools and Manufacture 46 (2) (2006) 98–106.

- [2] S. Pateloup, H. Chanal, E. Duc, Process definition of preformed part machining for taking benefit of parallel kinematic machine tool kinematic performances, *The International Journal of Advanced Manufacturing Technology* 58 (9) (2012) 869–883.
- [3] J. Merlet, *Parallel robots*, Vol. 128, Springer Science & Business Media, 2006.
- [4] G. Pritschow, C. Eppler, T. Garber, Influence of the dynamic stiffness on the accuracy of PKM, in: *Chemnitz Parallel Kinematic Seminar*, 2002, pp. 313–333.
- [5] T. Bonnemains, H. Chanal, C. Bouzgarrou, P. Ray, Definition of a new static model of parallel kinematic machines: Highlighting of overconstraint influence, in: *2008 IEEE/RSJ International Conference on Intelligent Robots and Systems*, 2008, pp. 2416–2421. doi:10.1109/IROS.2008.4650957.
- [6] W.-L. Liu, Y.-D. Xu, J.-T. Yao, Y.-S. Zhao, Methods for force analysis of overconstrained parallel mechanisms: a review, *Chinese Journal of Mechanical Engineering* 30 (6) (2017) 1460–1472.
- [7] K. J. Waldron, The constraint analysis of mechanisms, *Journal of Mechanisms* 1 (2) (1966) 101–114.
- [8] R. Ramesh, M. Mannan, A. Poo, Error compensation in machine tools — a review, *International Journal of Machine Tools and Manufacture* 40 (9) (2000) 1235–1256. doi:10.1016/s0890-6955(00)00009-2.
- [9] A. Majarena, J. Santolaria, D. Samper, J. Aguiar, Modelling and calibration of parallel mechanisms using linear optical sensors and a coordinate measuring machine, *Measurement Science and Technology* 22 (10) (2011) 105101. doi:10.1088/0957-0233/22/10/105101.
- [10] X. Yang, L. Wu, J. Li, K. Chen, A minimal kinematic model for serial robot calibration using POE formula, *Robotics and Computer-Integrated Manufacturing* 30 (3) (2014) 326–334. doi:10.1016/j.rcim.2013.11.002.
- [11] H. Chanal, J. B. Guyon, A. Koessler, Q. Dechambre, B. Boudon, B. Blaysat, N. Bouton, Geometrical defect identification of a scara robot

- from a vector modeling of kinematic joints invariants, *Mechanism and Machine Theory* 162 (2021) 104339.
- [12] J.-M. Renders, E. Rossignol, M. Becquet, R. Hanus, Kinematic calibration and geometrical parameter identification for robots, *IEEE Transactions on Robotics and Automation* 7 (6) (1991) 721–732. doi:10.1109/70.105381.
- [13] H. Chanal, E. Duc, J. Hascoët, P. Ray, Reduction of a parallel kinematics machine tool inverse kinematics model with regard to machining behaviour, *Mechanism and Machine Theory* 44 (7) (2009) 1371–1385. doi:10.1016/j.mechmachtheory.2008.11.004.
- [14] G. Alici, B. Shirinzadeh, A systematic technique to estimate positioning errors for robot accuracy improvement using laser interferometry based sensing, *Mechanism and Machine Theory* 40 (8) (2005) 879–906. doi:10.1016/j.mechmachtheory.2004.12.012.
- [15] G. Chen, H. Wang, Z. Lin, Determination of the Identifiable Parameters in Robot Calibration Based on the POE Formula, *IEEE Transactions on Robotics* 30 (5) (2014) 1066–1077. doi:10.1109/tro.2014.2319560.
- [16] L. Everett, M. Driels, B. Mooring, Kinematic modelling for robot calibration, in: *Proceedings. 1987 IEEE International Conference on Robotics and Automation*, Institute of Electrical and Electronics Engineers, 1987. doi:10.1109/robot.1987.1087818.
- [17] K. Fan, H. Wang, J. Zhao, T. Chang, Sensitivity analysis of the 3-PRS parallel kinematic spindle platform of a serial-parallel machine tool, *International Journal of Machine Tools and Manufacture* 43 (15) (2003) 1561–1569. doi:10.1016/s0890-6955(03)00202-5.
- [18] A. Mabire, P. Serré, M. Moinet, J.-F. Rameau, A. Clément, Computing clearances and deviations in over-constrained mechanisms, *Procedia CIRP* 75 (2018) 238–243.
- [19] R. Hartenberg, J. Denavit, A kinematic notation for lower pair mechanisms based on matrices, *Trans. ASME Journal of Applied Mechanics* (1955).

- [20] Y. Bai, H. Zhuang, Z. Roth, Experiment study of PUMA robot calibration using a laser tracking system, in: Proceedings of the 2003 IEEE International Workshop on Soft Computing in Industrial Applications, 2003. SMCia/03., IEEE, 2003. doi:10.1109/smcia.2003.1231359.
- [21] H. Chanal, F. Paccot, E. Duc, Sensitivity Analysis of an Overconstrained Parallel Structure Machine Tool, the Tripteor X7, Applied Mechanics and Materials 162 (2012) 394–402. doi:10.4028/www.scientific.net/amm.162.394.
- [22] A. Clément, C. Valade, A. Riviere, The ttrss: 13 oriented constraints for dimensioning, tolerancing & inspection, Series on Advances in Mathematics for Applied Sciences 45 (1997) 24–42.
- [23] T. Putschler, Kinematic transformation for the Exechon concept in the SI-NUMERIK 840D—parallel kinematic machines in research and practice (PKS'2006), Chemnitz, Germany (2006) 803–812.

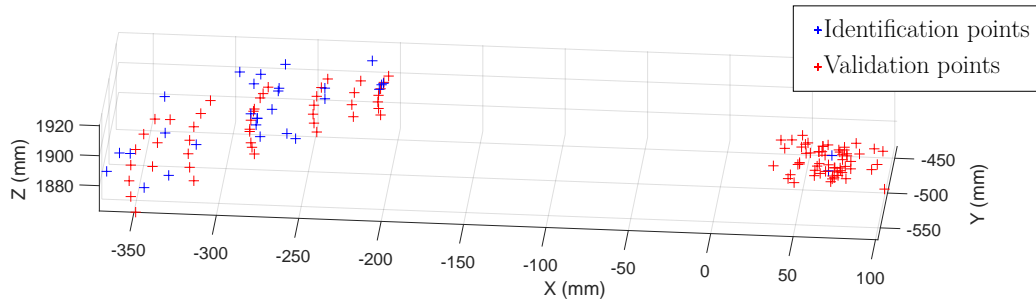


Figure 8: Measured points in the Tripteor X7 workspace. Red dots are identification points, blue dots are validation points

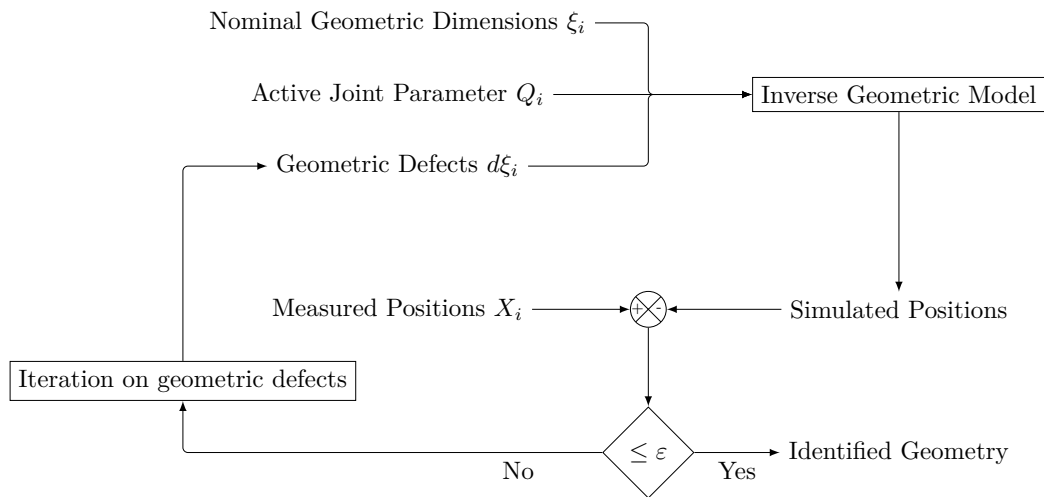


Figure 9: Diagramm of the identification Process used in this study

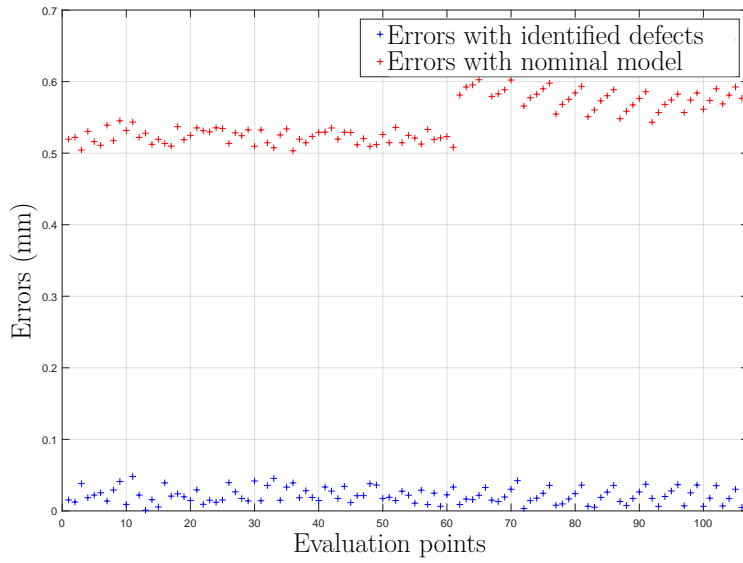


Figure 10: Norm of the error between measured and simulated position of the end effector of the Tripteor X7